Acknowledgment. This research was supported by NSF. The access to susceptibility data from the M.S. thesis of M. Ahmed and discussions with his thesis supervisor, Professor M. Mostafa, is gratefully acknowledged.

Supplementary Material Available: Listings of observed and calculated structure factor amplitudes for $(CH_3)_2CHNH_3CuCl_3$ in phases I and II (4 pages). Ordering information is given on any current masthead page.

Thermochromism in Copper(II) Halide Salts. 2. Bis(isopropylammonium) Tetrachlorocuprate(II)

Darrel R. Bloomquist,* Roger D. Willett, and Harold W. Dodgen

Contribution from the Department of Chemistry, Washington State University, Pullman, Washington 99164. *Received July 21, 1980*

Abstract: Bis(isopropylammonium) tetrachlorocuprate(II) is thermochromic, undergoing a first-order phase transition at T_{th} = 50 °C, changing from green to yellow. The structure of the high-temperature phase (orthorhombic, *Pnma*, a = 16.007 (4) Å, b = 12.262 (3) Å, and c = 7.784 (2) Å, Z = 4) has been determined and shown to contain distorted tetrahedral $CuCl_4^{2-}$ anions and disordered isopropylammonium cations. Cu–Cl distances range from 2.204 to 2.218 Å, with trans Cl–Cu–Cl angles = 134.3° and 135.3°. The previously determined room-temperature structure consists of ribbons of five- and six-coordinate copper ions based on the laminar $(RNH_3)_2CuCl_4$ structures. DSC studies yield ΔH_{th} = 2.9 kcal/mol and ΔS_{th} = 9.0 cal/(mol deg) for the transition. The value of ΔS_{th} is consistent with the disorder of the cations and the drastic rearrangement of the cationic structure. Broad-line ^1H NMR measurements show that the anion disorder is dynamic in nature. The second moment of the NMR line drops discontinuously from 7.8 to 4.8 G^2 at the phase transition. This is in quantitative agreement with theoretical second moments based on the disorder observed in the high-temperature phase. The EPR spectrum also shows a discontinuous change at the phase transition. Magnetic susceptibility studies on the quenched high-temperature phase show the existence of extremely weak antiferromagnetic coupling between the $CuCl_4^{2-}$ ions, probably occurring via hydrogen bonding. The data all strongly support the hypothesis that the thermochromism in copper halides is driven entropically by the onset of dynamic disorder of the organic cations. The weakening of the hydrogen bonding destabilizes the low-temperature stereochemistry, allowing, in most cases, the copper halide salt to distort toward tetrahedral geometry.

In a series of papers, we have investigated the phenomenon of thermochromism in copper halide salts. In particular, emphasis has been on those salts in which the color change is associated with a change in stereochemistry brought about by the presence of a structural phase transition. Spectroscopically, it has shown that the color change is associated with a relaxation of the stereochemistry from a square-planar (or square-pyramidal or square-bipyramidal) geometry toward a tetrahedral geometry.[1-3] Structurally, this has been verified for $(PhCH_2NH_2CH_3)_2CuCl_4$.[4] A counter example to this was shown to exist in $[(CH_3)_2CHNH_3]CuCl_3$, where the coordination geometry *increased* from square pyramidal to square bipyramidal.[5] A subsequent study of the corresponding bromide salt showed the existence of an additional phase in which a distortion toward tetrahedral geometry apparently exists.[6] In the latter studies, it was shown that the phase transitions were driven entropically by the onset of dynamic disorder of the organic cations. Hydrogen bonding is thus weakened in the high-temperature phase, allowing electrostatic effects to dominate over crystal field stabilization in the determination of the stereochemistry.

In this paper, the structure and magnetic behavior of the high-temperature phase of $[(CH_3)_2CHNH_3]_2CuCl_4$, henceforth $(IPA)_2CuCl_4$, is reported, along with a DSC, ^1H NMR, and EPR study of the phase transition.

Experimental Section

Crystals of the room-temperature phase (phase II) of $(IPA)_2CuCl_4$ grow as fine straw green needles from methanol, ethanol, or aqueous solutions containing stoichiometric amounts of the hydrochloride salt of isopropylamine and cupric chloride dihydrate as described by Remy and Laves.[7] Much larger single crystals of higher purity can be obtained upon slow evaporation from *n*-propyl alcohol. This compound can also be prepared as a fine powder by adding ether to a saturated ethanolic solution. The high-temperature phase (phase I) grows as yellow, rectangular platelets from hot alcoholic solutions.

DTA and DSC measurements were carried out on a Du Pont 900 thermal analyzer. The ^1H continuous-wave NMR measurements were made with an instrument with a phase-sensitive detection design incorporating a PAR lock-in amplifier and a Varian V4210A variable-frequency R-F unit. Data were recorded, while sweeping the magnetic field, with a FabriTech 1052 LSH 1024 point signal averager interfaced with a Motorola microprocessor previously described. The EPR spectra were recorded on a Varian E-3 spectrometer. A liquid-circulation temperature-control system designed to fit either instrument was used for precise temperature regulation from 20 to 100 °C.[8] Dow Corning 200 electronic fluid functions satisfactorily as the thermal liquid for EPR measurements while perfluorotributylamine was found to be the ideal liquid for ^1H NMR experiments. Magnetic susceptibility studies were carried out on a PAR vibrating sample magnetometer. The same techniques previously described were utilized for obtaining data on the quenched high-temperature phase.[5] A 0.1086-g sample was used and diamagnetic corrections (-126×10^{-6} emu/mol) and TIP paramagnetic corrections (60×10^{-6} emu/mol) were applied.

The crystalline properties of a single crystal of $(IPA)_2CuCl_4$ are destroyed during the phase transition. Freshly prepared room-temperature

* To whom correspondence should be addressed at Hewlett-Packard, Disc Memory Division, Boise, Idaho 83707.

(1) R. D. Willett, J. A. Haugen, J. Lebsack, and J. Morrey, *Inorg. Chem.*, **13**, 2510 (1974).
(2) G. Marcotrigiano, L. Menabue, and G. C. Pellacani, *Inorg. Chem.*, **15**, 2333 (1976).
(3) R. D. Willett, J. R. Ferraro, and M. Choca, *Inorg. Chem.*, **13**, 2919 (1974).
(4) R. L. Harlow, W. J. Wells, III, G. W. Watt, and S. H. Simonsen, *Inorg. Chem.*, **13**, 2106 (1974).
(5) S. A. Roberts, D. R. Bloomquist, R. D. Willett, and H. W. Dodgen, *J. Am. Chem. Soc.*, to be submitted for publication.
(6) D. R. Bloomquist, R. D. Willett, and H. W. Dodgen, *J. Am. Chem. Soc.*, to be submitted for publication.
(7) H. Remy and G. Laves, *Ber.*, **66**, 401 (1933).
(8) D. R. Bloomquist and H. W. Dodgen, to be submitted for publication.

0002-7863/81/1503-2610$01.25/0

Table I. Final Thermal and Positional Parameters for $(IPA)_2CuCl_4$ Phase I

atom	*x*	*y*	*z*	*U*(1,1)	*U*(2,2)	*U*(3,3)	*U*(1,2)	*U*(1,3)	*U*(2,3)
Cu	0.7559 (2)	0.7500	0.0706 (2)	0.101 (3)	0.158 (7)	0.0176 (5)	0.0	−0.001 (1)	0.0
Cl(1)	0.9364 (5)	0.7500	0.0774 (4)	0.095 (7)	0.62 (3)	0.020 (1)	0.0	0.000 (3)	0.0
Cl(2)	0.6360 (5)	0.7500	0.9668 (4)	0.121 (8)	0.47 (2)	0.021 (1)	0.0	−0.014 (3)	0.0
Cl(3)	0.7248 (5)	0.0120 (7)	0.1172 (4)	0.259 (9)	0.15 (1)	0.040 (1)	0.012 (8)	−0.000 (3)	−0.014 (3)
N(A)	0.393 (2)	0.7500	0.026 (1)	0.19 (3)	0.34 (7)	0.015 (4)	0.0	−0.00 (1)	0.0
C(1A)	0.366 (3)	0.7500	0.114 (3)	0.09 (4)	0.6 (1)	0.029 (8)	0.0	0.00 (1)	0.0
C(2A)	0.250 (3)	0.7500	0.129 (2)	0.17 (4)	0.9 (1)	0.029 (6)	0.0	0.00 (2)	0.0
C(3A)	0.437 (3)	0.7500	0.176 (2)	0.26 (6)	0.6 (1)	0.025 (7)	0.0	−0.02 (2)	0.0
N(B)	0.443 (2)	0.2500	0.401 (1)	0.16 (3)	0.40 (7)	0.008 (3)	0.0	0.004 (8)	0.0
C(1B)	0.018 (3)	0.2500	0.170 (2)	0.16 (5)	0.6 (1)	0.024 (8)	0.0	0.04 (2)	0.0
C(2B)	0.105 (3)	0.159 (5)	0.170 (2)	0.11 (4)	0.5 (2)	0.021 (7)	0.17 (6)	−0.01 (1)	−0.00 (2)
C(3B)	0.458 (3)	0.2500	0.252 (2)	0.21 (5)	0.9 (1)	0.022 (6)	0.0	−0.01 (2)	0.0

crystals are transparent green and extinguished sharply under a polarizing microscope whereas crystals that have been cycled through the phase transition are opaque and show no sign of a polarization axis. When a long needle crystal is mounted on one end and heated through the transition, the free end of the crystal moves enough to detect visually, demonstrating the severity of the structural rearrangement.

Since $(IPA)_2CuCl_4$ decomposes at the melting temperature, the only method of obtaining single crystals of the high-temperature phase is by recrystallization from a solvent above the transition temperature. Slow evaporation to dryness of an ethanol solution of $(IPA)_2CuCl_4$ maintained at 70 °C provided a solid yellow mass from which single crystals could be isolated. Clear yellow crystals examined on a hot stage of a polarizing microscope were found to extinguish sharply.

In order to obtain an X-ray diffraction data set, it was necessary to mount a single crystal, transfer it to the diffractometer, and collect data without allowing the crystal to cool below the transition temperature. This was accomplished by mounting a single crystal using hot cyanoacrylate glue, and rapidly transferring it to the diffractometer, equipped with a gas-flow temperature controller adjusted to direct a stream of warm air (70 °C) at the crystal. No attempt was made to shield the crystal from the environment.

Background was measured for 15 s before and after each scan. Systematic extinctions ($0kl$, $k + l = 2n + 1$, and $hk0$, $h = 2n + 1$) for the orthorhombic unit cell corresponded to the nonstandard space groups *Pnma* or $Pn2_1a$. Accurate lattice constants were determined from a least-squares refinement of 12 high angle reflections to be $a = 16.007$ (4) Å, $b = 12.262$ (3) Å, and $c = 7.784$ (2) Å with $Z = 4$ (λ(Mo Kα) = 0.710 69 Å.) A total of 684 reflections were collected for $4° \leq 2\theta \leq 40°$ by using zirconium-filtered Mo Kα radiation. Data were collected by using a 1.8° θ–2θ step scan with a step size of 0.05° and 3.0 seconds counting time per step. Three standard peaks, monitored every 41 reflections, showed a 45% linear decay during the data collection. Visual inspection of the crystal revealed severe surface decomposition. Data were corrected for linear decay and Lorentz polarization, but absorption corrections were not applied. The standard deviation of each reflection was calculated as $\sigma^2(I) = TC + BG + (0.03I)$ where TC is total counts, BG is background counts, and I is net intensity (TC − BG).

Structure Solution

The coordinates for the $CuCl_4^{2-}$ anion were determined by using MULTAN and confirmed by analysis of a Patterson map. Both IPA cations were easily located on subsequent Fourier and difference Fourier maps. No attempt was made to include hydrogen atoms in the refinement. All atoms were located on or disordered across the mirror planes except for Cl(3). Maximum intensity for all of the atoms in the two crystallographically independent IPA ions appeared on the mirror planes with large thermal motion normal to the plane except for C(2B), which showed resolvable disorder across the mirror plane.

Structural refinement was completed by using a data set totaling 564 with reflections of intensity less than 2σ omitted. Atoms on the mirror planes were refined by using anisotropic thermal parameters restricted by mirror symmetry. Thermal parameters for Cl(3) and C(2B) were varied anisotropically with no restrictions. Final refinement proceeded to a conventional residual of $R = 0.119$ ($R = (\sum||F_o| - |F_c||/\sum|F_o|)$ and a weighted residual of 0.079 ($R_w = [\sum w(F_o - F_c)^2]^{1/2}/(\sum wF_o^2)^{1/2}$, where $w = 1/\sigma^2(F)$). Final positional and thermal parameters are given in Table I and bond distances and angles are summarized in Table II. A portion of the unit cell is drawn in Figure 1 and stereo ORTEP drawings of the unit cell viewed normal to and parallel with the mirror planes are shown in Figure 2. All crystallographic calculations were carried out by using a local program library.[9,10]

Table II. Bond Distances (Å) and Angles (Deg) for $(IPA)_2CuCl_4$ (70 °C)

atoms	distances	atoms	angles
	$CuCl_4$ Geometry		
Cu–Cl(1)	2.217 (7)	Cl(1)–Cu–Cl(2)	134.3 (3)
Cu–Cl(2)	2.218 (7)	Cl(1)–Cu–Cl(3)	99.0 (2)
Cu–Cl(3)	2.204 (5)	Cl(2)–Cu–Cl(3)	98.0 (2)
		Cl(3)–Cu–Cl(3)	135.3 (3)
	IPA Ion A Geometry		
C(1A)–N(A)	1.45 (4)	N(A)–C(1A)–C(2A)	112 (3)
C(1A)–C(2A)	1.44 (4)	N(A)–C(1A)–C(3A)	126 (3)
C(1A)–C(3A)	1.31 (4)	C(2A)–C(1A)–C(3A)	122 (4)
	IPA Ion B Geometry		
C(1B)–N(B)	1.47 (4)	N(B)–C(1B)–C(2B)	122 (3)
C(1B)–C(2B)	1.28 (3)	N(B)–C(1B)–C(3B)	110 (3)
C(1B)–C(3B)	1.45 (4)	C(2B)–C(1B)–C(3B)	115 (3)
C(2B)–C(2B)	1.41 (8)	C(2B)–C(1B)–C(2B)	67 (4)
	Nitrogen–Chlorine Distances		
N(B)–Cl(1)	3.19 (2)	N(A)–Cl(2)	3.13 (2)
N(B)–Cl(3)	3.26 (2)	N(A)–Cl(3)	3.28 (2)

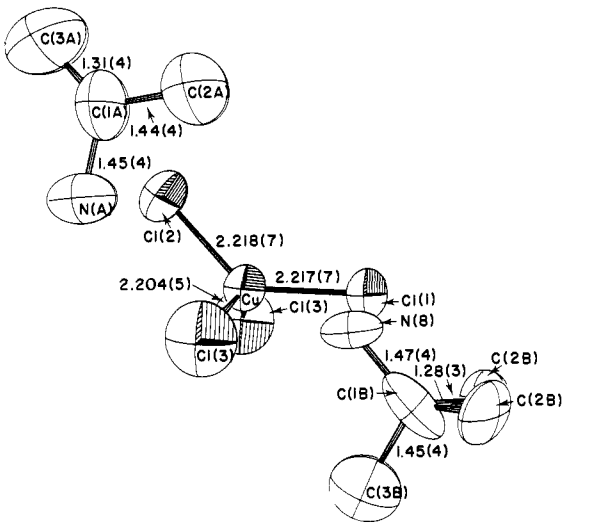

Figure 1. An ORTEP drawing of one asymmetric unit of $(IPA)_2CuCl_4$ phase I with atoms and bond distances labeled.

Thermal Analysis

As the compound is heated, a discontinuous phase transition occurs accompanied by a change in color to golden yellow. The temperature at which the thermochromism occurs depends on sample purity, heating rate, particle size, and previous thermal history, making it difficult to define a precise transition temperature. A DTA scan run at 10°/min for a pure powdered sample of $(IPA)_2CuCl_4$ grown from a propanol solution shows a very sharp endotherm at the phase transition and a reasonably

(9) D. N. Anderson, Ph.D. Thesis, Washington State University, 1971.

(10) R. E. Caputo, Ph.D. Thesis, Washington State University, 1976.

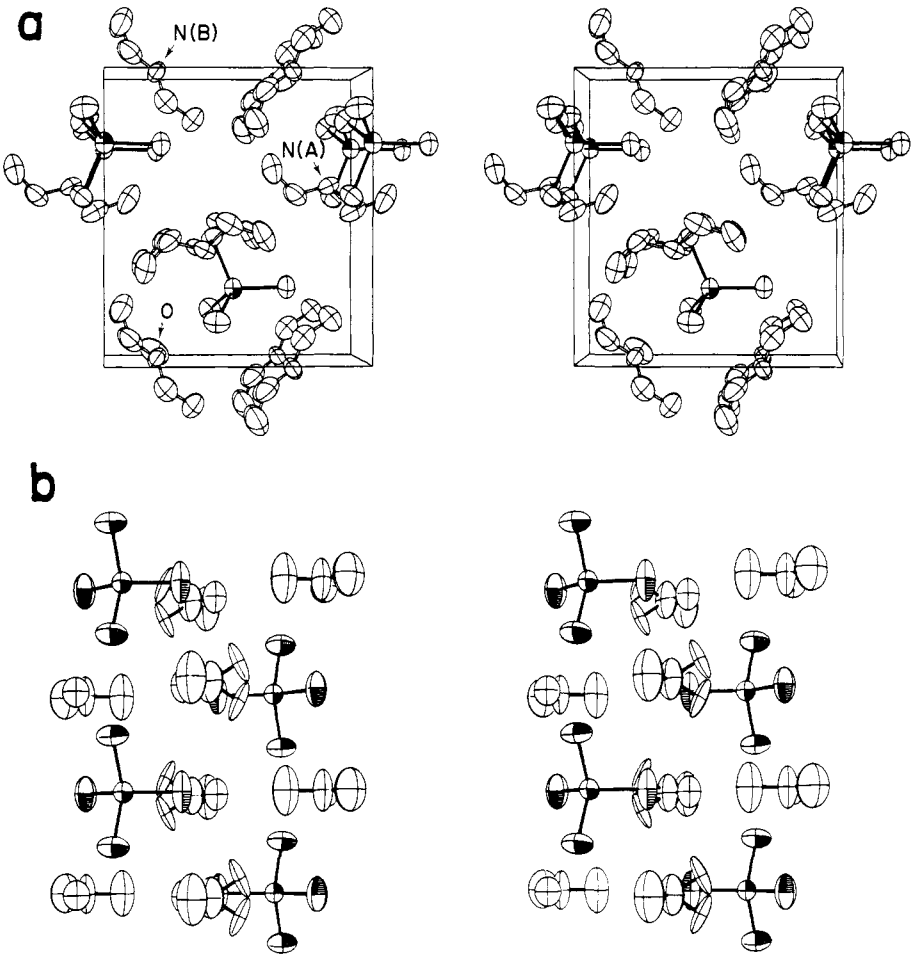

Figure 2. Stereo ORTEP drawings of the unit cell of $(IPA)_2CuCl_4$ viewed (a) normal to and (b) parallel with the mirror planes. The $CuCl_4^{2-}$ ion is drawn with crosshatching, and the IPA ions are drawn as solid ellipsoids. IPA ion B can be distinguished from ion A by the disorder shown for C(2B).

sharp melting point (see Figure 1). For a pure sample, it is not unusual for the DTA phase transition to occur 10–15 °C above the actual equilibrium temperature due to superheating. The temperature at which the discontinuity in NMR behavior occurs (50 °C) for a finely powdered sample that has previously been heated above the transition is reproducible and is reported as the transition temperature. The NMR temperature is chosen since this experiment allows adequate time for thermal equilibrium with precise temperature control. Integration of the endotherm of a DSC scan using a scan rate of 5°/min yields a value of ΔH = 2.9 (0.1) kcal/mol for the transition corresponding to ΔS = 9.0 (0.3) cal/(mol deg). $(IPA)_2CuCl_4$ melts at 155 (5) °C with ΔH_{melt} = 6.5 (0.2) kcal/mol.

Crystal Structures

Tetrachlorocuprate(II) salts of a primary ammonium ion typically crystallize in a two-dimensional layer structure with layers separated by the organic cations.[11] The crystal structure of the room-temperature phase (phase II) of $(IPA)_2CuCl_4$,[12] however, contains an unusual system of distorted square-planar $CuCl_4^{2-}$ ions arranged in a two-dimensional ribbon-like chain. The structure contains four crystallographically unique $CuCl_4^{2-}$ ions forming two inequivalent chains running along the crystallographic a axis. Each ribbon contains a planar $CuCl_4^{2-}$ anion bridged by a pair of $CuCl_4^{2-}$ anions which have a small tetrahedral distortion. These ribbons are sheathed by the IPA cations. As the pressure is increased, a transformation occurs to the more familiar layered A_2MX_4 structure similar to that of methylammonium tetrachlorocuprate(II).[3] As the temperature is raised at ambient pressure, a thermochromic phase transition to the third phase (phase I) occurs.

The four unique $CuCl_4^{2-}$ anions of the room-temperature phase become equivalent above the phase transition. In phase I, the $CuCl_4^{2-}$ anions are isolated and have distorted tetrahedral geometry with somewhat shorter than normal Cu–Cl bond lengths (Cu–Cl(average) = 2.211 Å). these distances are artificially shortened due to the large thermal motion of the chlorine atoms. A parameter often used to characterize complexes containing the $CuCl_4^{2-}$ ion is θ, defined as the average of the trans angles in the complex. The average value of θ in the low-temperature phase is 167.7° while θ is 134.8° in phase I. This is in the range associated with moderately strong hydrogen bonding.[1] The change in geometry of the $CuCl_4^{2-}$ chromophore from square planar to tetrahedral is responsible for the drastic change in color associated with the phase transition.

The presence of a pyramidal IPA ion on a mirror plane indicates disorder, presumably dynamic in nature. Thermal parameters of cation A normal to the mirror plane are large enough to account for a twofold hindered rotation about an axis defined by the average N(A)–C(1A) bond. In cation B, a similar flipping motion is postulated, except the flipping angle is less than 180°. a flipping motion of 135° about the average N(B)–C(1B) bond accounts for the disorder seen in C(2B). Anisotropic thermal ellipsoids provide a rather poor model for this type of motion accounting for the short bond distances and large bond angles reported in Table II.

NMR Studies

Figure 3 summarizes the NMR data obtained for $(IPA)_2CuCl_4$ from 20 to 74 °C. At the phase transition temperature, a discontinuous drop in second moment from 7.8 (0.5) G^2 to 4.8 (0.2) G^2 is observed. This substantiates the anticipation of a dynamic

(11) J. P. Stedman and R. D. Willett, *Inorg. Chim. Acta*, **4**, 367, (1970). D. W. Phelps, D. B. Losee, W. E. Hatfield, and D. J. Hodgson, *Ingor. Chem.*, **15**, 3147 (1976). B. Morosin, P. Fallon, and J. S. Valentine, *Acta Crystallogr. Sect. B*, **B31**, 2220, (1975). K. P. Larsen, *Acta Chem. Scand.*, **28**, 194 (1974).
(12) D. N. Anderson and R. D. Willett, *Inorg. Chim. Acta*, **8**, 167 (1974).

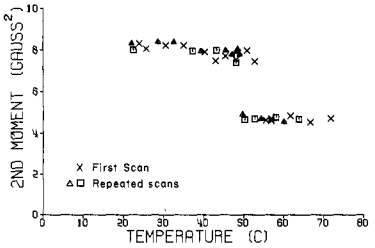

Figure 3. NMR second moment versus temperature for $(IPA)_2CuCl_4$. Notice that the low-temperature phase (phase II) superheats by 5 °C the first time a fresh sample is heated.

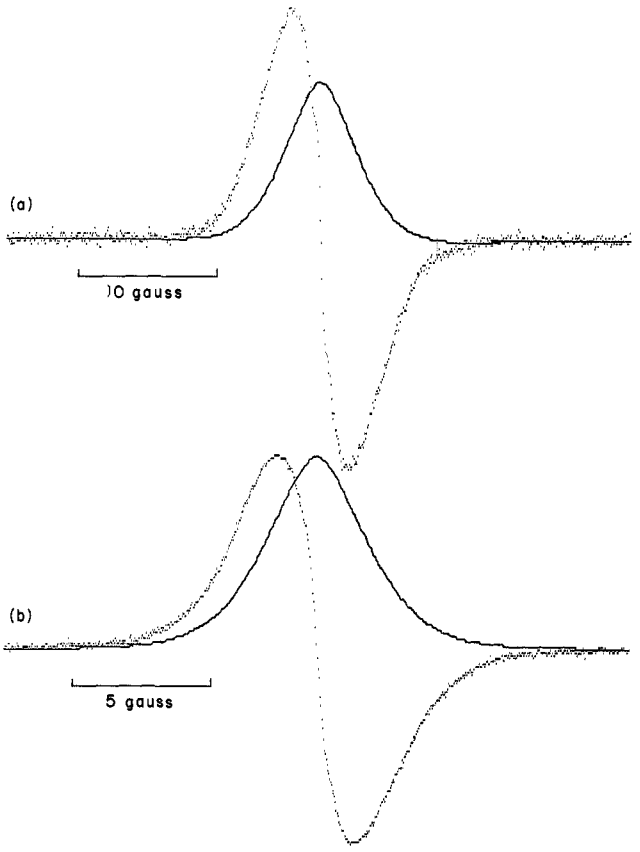

Figure 4. Examples of NMR derivative spectra for $(IPA)_2CuCl_4$ below and above the phase transition (integrated line shape is drawn as a solid line). The spectrum in phase II at 50.7 °C is shown as (a) while (b) is phase I at 56.8 °C. Notice the difference in horizontal scale.

disorder of the IPA ion. The drop in second moment is somewhat larger (38%) than that observed for the twofold disorder in $IPACuBr_3$ (30%).[6]

It is possible to calculate the change in NMR second moment for IPA ions undergoing the type of disorder deduced from the X-ray study. The Van Vleck equation for the second moment of a single crystal[13] is

$$M_2 = \frac{3}{2}\frac{I(I+1)g^2\beta^2}{N}\sum_{j>k}(3\cos^2\theta_{jk}-1)^2 r_{jk}^{-6}$$

where r_{jk} is the internuclear distance between the jth and the kth atoms and θ is the angle between the magnetic field and the vector $\vec{r}_{jk}$. The contribution of off-resonance nuclei has been omitted. For a powder, this is averaged over all crystal orientations, yielding

$$M_2(\text{powder}) = \frac{6}{5}\frac{I(I+1)g^2\beta^2}{N}\sum_{j>k} r_{jk}^{-6}$$

In the presence of rapid thermal motion, the dipolar interaction must be averaged over all possible motions prior to the calculation of the second moment and before performing the powder average,[14] i.e.

$$M_2 = \frac{3}{2}\frac{I(I+1)g^2\beta^2}{N}\sum_{j>k}\left[\frac{\langle 3\cos^2\theta_{jk}-1\rangle_{\text{thermal}}}{r_{jk}^3}\right]^2$$

where $\langle\ \rangle_{\text{thermal}}$ denotes the average over all motions. For a powder, this can be written as

$$M_2(\text{powder}) = \frac{3}{2}\frac{I(I+1)g^2\beta^2}{N}\sum_{j>k}\left\langle\left[\frac{\langle 3\cos^2\theta_{jk}-1\rangle_{\text{thermal}}}{r_{jk}^3}\right]^2\right\rangle_{\text{powder}}$$

where $\langle\ \rangle_{\text{powder}}$ implies the powder average over all orientations. This is too complicated to evaluate rigorously for the complete crystal structure. It is feasible, however, to consider this solely for the motion of a single IPA ion, ignoring explicitly effects due to neighboring ions, since then the r_{jk} terms can be pulled outside of the thermal (and powder) average.

For single stationary IPA cation, the second moment is given by

$$M_2(\text{powder}) = 71.62\sum_{j>k} r_{jk}^{-6}$$

When the second moment is reduced due to motion, the results can be expressed in terms of reduction factors (R_{jk})

$$M_2(\text{powder}) = 71.62\sum_{j>k} R_{jk} r_{jk}^{-6}$$

To simplify calculations, all angles are assumed to be tetrahedral and proton–proton distances within the methyl groups and the NH_3 group are taken to be 1.79 Å.[14] This corresponds to a C–H or N–H bond distance of 1.10 Å. A value of 1.50 Å is used as the bond distance for C–C and C–X bonds in agreement with crystal structure results. It was assumed that the methyl groups were undergoing hindered threefold rotation at room temperature.

The predicted second moment for the low-temperature phase of $(IPA)_2CuCl_4$ is 11.62 G^2 (no flipping motion), and the second moment above the transition temperature is predicted to be 6.82 G^2, the average for one IPA ion undergoing a 180° hindered rotation (7.95 G^2) while the other ion is flipping between two sites 135° apart (5.69 G^2). Although the observed second moments are somewhat smaller than the calculated values, the observed drop in second moment (38%) is in good agreement with the calculated decrease of 41% for the motions postulated. The disagreement between observed and calculated second moments is not unexpected in that intermolecular dipolar interactions and intramolecular torsional and vibrational motions have been neglected in the calculations.

EPR Studies

For a single crystal of the room-temperature phase of $(IPA)_2CuCl_4$, the EPR spectrum contains two separate resonance lines, each showing an angular dependence corresponding to the two isolated two-dimensional ribbons within the structure. A detailed study of the anisotropic **g** tensor and line width behavior of each ribbon has been published.[15] For a powdered sample, the **g** tensors for both ribbons are averaged and a single, nearly symmetric resonance line is observed since the line width is nearly as large as the **g** tensor anisotropy.

As a fresh, powdered sample of $(IPA)_2CuCl_4$ is slowly heated from 20 °C to a temperature just below the phase transition temperature, no significant change in line shape, line width, or resonance frequency is observed. Above 55 °C, the symmetric line vanishes and a broader asymmetric line corresponding to the high-temperature phase appears. The temperature at which the

(13) J. H. Van Vleck, *Phys. Rev.*, **74**, 1168 (1948).

(14) E. R. Andrew and R. Bersohn, *J. Chem. Phys.*, **18**, 159 (1950).
(15) D. R. Bloomquist and R. D. Willett, *J. Phys. Chem. Solids*, submitted for publication.
(16) C. P. Landee, S. A. Roberts, and R. D. Willett, *J. Chem. Phys.*, **68**, 4574 (1978).

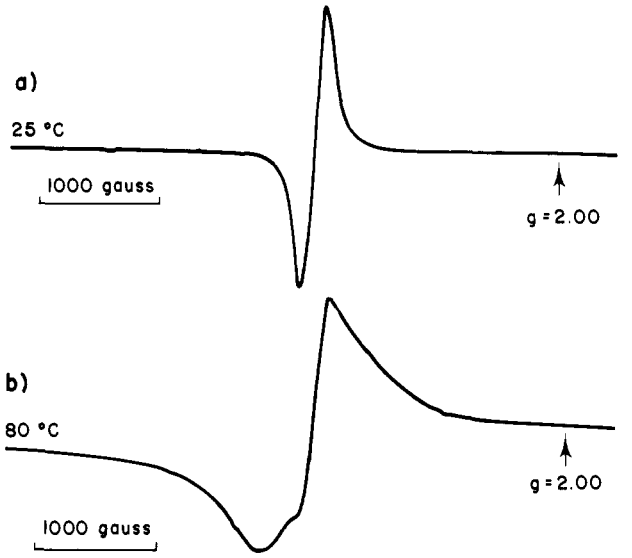

Figure 5. Representative EPR spectra for a powdered sample of $(IPA)_2CuCl_4$ (a) below the phase transition and (b) above the transition temperature. Scale and relative position are shown with each spectra.

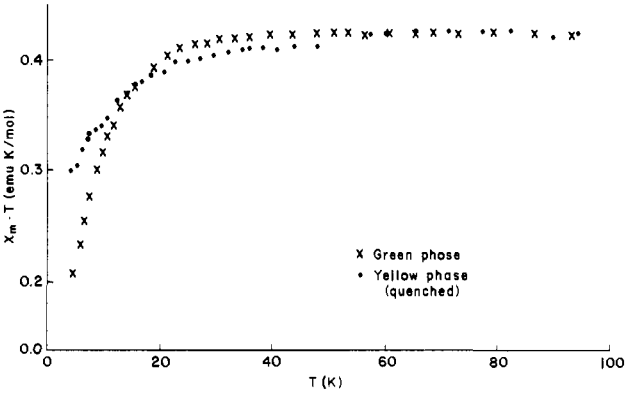

Figure 6. Magnetic susceptibility data for both phases of $(IPA)_2CuCl_4$ plotted as $\chi_m T$ vs. T.

discontinuity occurs in the EPR experiment is the same as the temperature at which the NMR line narrows the first time a fresh sample is heated. Examples of EPR spectra obtained above and below the phase transition for a powdered sample are shown in Figure 5. The peak to peak line width shows little temperature dependence above or below the transition temperature, but changes discontinuously from 200 to 530 G at T_{th}. The absence of premonitory behavior near the phase transition is typical of an ideal first-order phase transition.

Magnetic Susceptibility Studies

The magnetic susceptibility data have been obtained for both phases of $(IPA)_2CuCl_4$ as shown in Figure 6. Magnetic data for the room-temperature phase of $(IPA)_2CuCl_4$ can be fit satisfactorily by using a model for Ising-coupled Heisenberg trimers with a ferromagnetic intratrimer coupling of J/k = 45 K and an antiferromagnetic intertrimer interaction with $J'/K = -5.5$ K.[14] Data above 120 K have been fit to a Curie–Weiss law behavior $(1/\chi = (T - \Theta)/C)$ with $C = 0.43$ (2) (corresponds to $g = 2.10$ (2) and $\Theta/k = +23$ (2) K) consistent with a ferromagnetic intratrimer interaction.

In the high-temperature phase, the $CuCl_4^{2-}$ anions are isolated with distorted tetrahedral geometry and no significant exchange interactions are anticipated. A Curie–Weiss plot of the data collected using a sample of the quenched high-temperature phase of $(IPA)_2CuCl_4$ is presented in Figure 7. The data lie on a straight line nearly passing through the origin ($\Theta/k \leq 1$ K), indicating nearly paramagnetic behavior. In Figure 6, an apparent discontinuity in the quenched phase data occurs between 40 and 60

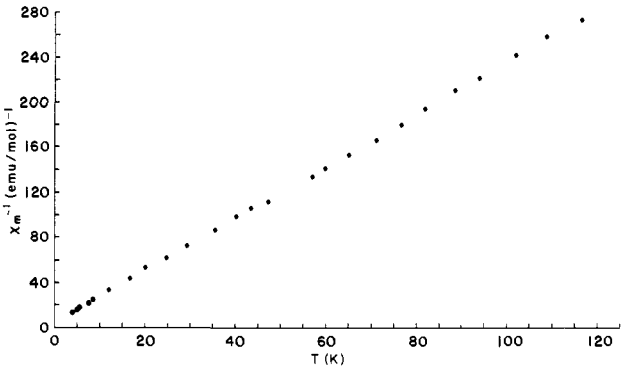

Figure 7. Curie–Weiss plot for the magnetic data of the quenched phase of $(IPA)_2CuCl_4$ showing paramagnetic behavior.

K, indicating reversion of the quenched phase back to the more stable room-temperature phase.

Discussion

The phenomena of thermochromism in copper halide salts appears to be strongly associated with the dynamics of the organic counterions. The stereochemistry of the copper ions in these salts represents a delicate balance between crystal field stabilization effects, favoring a square-planar geometry, and ligand–ligand electrostatic repulsions, favoring a distorted tetrahedral geometry. Excess electrostatic charge on the halide ions can be neutralized in two ways: through bridge formation with neighboring copper ions or through hydrogen bonding with the organic counterions. If the electrostatic charge cannot be adequately compensated, the copper halide complex will relax its coordination geometry toward tetrahedral. An ideal example of the use of hydrogen bonding to stabilize the square-planar coordination geometry is found in $(PhC_2H_4NH_2CH_3)_2CuCl_3$,[4] where the anion changes directly from an isolated square-planar $CuCl_4^{2-}$ to a distorted tetrahedral anion at the phase transition.

$(IPA)_2CuCl_4$ presents an interesting variation on this theme. The high pressure phase assumes the laminar $(RNH_3)_2CuCl_4$ structure, in which the copper halide sublattice forms a particularly stable arrangement, with two of the chloride ions involved in asymmetric Cu–Cl···Cu bridge formation and the ammonium ions forming two strong hydrogen bonds to each of the two nonbridging and one to the bridging halide. The steric bulk of the two methyl groups in the IPA ion, however, make the laminar lattice energetically unfavorable for $(IPA)_2CuCl_4$ at normal pressures, and the lattice distorts to form a complex linear chain structure, which can be visualized as a ribbon cut from the laminar lattice by breaking some of the long Cu···Cl interactions. The IPA ions sheath the ribbons, continuing to form strong N–H···Cl hydrogen bonds. The copper ions at the center of each ribbon retain their 4 + 2 geometry, and the $CuCl_4^{2-}$ moiety assumes a planar geometry. On the other hand, the $CuCl_4^{2-}$ ions at the edge of each ribbon now are forced to assume a 4 + 1 geometry and show a definite distortion toward tetrahedral geometry. The transition from the pressure stable to room-temperature phase does not involve any disorder, so the driving force is primarily enthalpic (as opposed to entropic) in nature.

In the transition to the high-temperature phase, the hydrogen bonding is weakened due to the amount of dynamic disorder of the IPA cations. The $CuCl_4^{2-}$ anions on the edge of the ribbon continue their distortion. This causes the remaining long Cu···Cl interactions to be weakened, and the central $CuCl_4^{2-}$ ion also distorts toward the final D_{2d} flattened tetrahedral coordnation geometry observed in the high-temperature phases. The driving force of this transition is clearly entropic in nature.

From this description, it is clear that there is little, if any, relationship between the phase II and phase I structures. This accounts for the loss of crystalline integrity upon heating or cooling a crystal through the phase transition. The first-order nature of the phase transition, as deduced from the NMR and EPR experiments, is also very understandable. No symmetry elements present in phase I are retained in phase II (the location of the

$\bar{1}$ element present in phase II is different than the location of the $\bar{1}$ element in phase I), so the transition cannot be second order.

The entropy change per IPA cation, 4.5 cal/(mol deg), is 18% larger than the increase in entropy observed during the phase transition in $IPACuCl_3$ and $IPACuBr_3$.[5,6] In the later cases, this increase was associated with the onset of a simple twofold disorder. However, the copper halide lattice takes on a more compact form during that process, the observed entropy should be slightly less than that anticipated for only disorder of the anions. In $(IPA)_2CuCl_4$, on the other hand, the copper halide lattice becomes less orderly. Hence, the 18% difference in ΔS_{th} value seems quite reasonable and in accord with the structural characteristics of the transition.

Supplementary Material Available: A listing of observed and calculated structure factor amplitudes for $[(CH_3)_2CHNH_3]_2CuCl_2$ (2 pages). Ordering information is given on any current masthead page.

Thermochromism in Copper Halide Salts. 3. Isopropylammonium Tribromocuprate(II)

Darrel R. Bloomquist* and Roger D. Willett

Contribution from the Department of Chemistry, Washington State University, Pullman, Washington 99164. *Received July 21, 1981*

Abstract: Isopropylammonium tribromocuprate(II), $(CH_3)_2CHNH_3CuBr_3$, undergoes two structural transitions above room temperature. The room-temperature phase (phase III), containing linear chains of $Cu_2Br_6^{2-}$ dimers, is isomorphous with the corresponding chloride salt. The triclinic bromide salt, $P\bar{1}$, a = 12.135 (6) Å, b = 8.199 (4) Å, c = 6.397 (3) Å, α = 78.79 (3)°, β = 124.72 (2)°, γ = 117.22 (3)°, was refined to a final R value of 0.054. The intermediate phase (phase II) appears to be isomorphous with the linear chain structure of the high-temperature phase of the chloride salt. The structure of phase I is unknown. The ^1H NMR second moment decreases by 30% at the first phase transition and an additional 20% at the second phase transition. The first transition corresponds to a dynamic twofold disorder of the IPA cations in phase II; additional motion exists in phase I. The magnetic susceptibility of phase III is consistent with the observed dimeric structure, with a ground-state singlet approximately 190 K below the excited triplet state. The susceptibility of quenched phase II shows the expected strong ferromagnetic intrachain interactions. In quenched phase I, the salt shows predominant antiferromagnetic interaction, with the a transition to a weak ferromagnetic ordered state at 6 K. This indicates that the linear chain structure in phase II does not persist into phase I. Instead, a monobridged chain of $CuBr_4^{2-}$ tetrahedra is postulated for phase I.

Copper halides salts exhibit a wide variety of structural geometries, including distorted tetrahedral geometry as in Cs_2CuCl_4,[1] square pyramidal in $(C_6H_{11}NH_3)CuCl_3$,[2] squares bipyramidal in $(RNH_3)_2CuCl_4$ salts,[3] square planar in $(C_6H_5CH_2CH_2NH_2CH_3)_2CuCl_4$,[4] and trigonal bipyramidal in $Co(NH_3)_6CuCl_5$.[5] In addition, linkage isomerization leads to an incredibly wide array of structural geometries, even with a single counterion, as exhibited by the sequence $[(CH_3)_3NH]_2Cu_4Cl_{10}$,[6] $[(CH_3)_3NH]_3Cu_2Cl_7$,[7] $[(CH_3)_3NH]_2CuCl_4$, and $[(CH_3)_3NH]_3CuCl_5$.[8] The relatively comparable energies of these geometries is demonstrated by the observation of several geometries in a single salt such as distorted tetrahedral and square-bipyramidal ions in $[(CH_3)_3NH]_3Cu_2Cl_7$,[9] three distorted tetrahedral ions in $[(CH_3)_2CHNH_3]_2CuCl_4$,[10] and distorted tetrahedral, square pyramidal, and square bipyramidal in $(N(2amet)pipzh_3)_4Cu_5Cl_{22}$ where $N(2amet)pipzH_3$ is the N-2-ammoniummethylpiperazinium cation.[11] The ease of interconversion between these geometries is testified to by the phenomenon of thermochromism, where the salts undergo first-order structural phase transitions involving a change in coordination geometry.[4,12-14] Spectroscopic studies indicate that these generally involve a transformation toward tetrahedral geometries in the high-temperature phase. It is postulated that the low-temperature structure is stabilized by cation–halide hydrogen-bonding interactions. This is weakened by the onset of dynamic disorder in the high-temperature phase, allowing the electrostatic repulsion to force the complex to distort toward a tetrahedral geometry.

An exception to this trend is found in $(CH_3)_2CHNH_3CuCl_3$, abbreviated $IPACuCl_3$, in which the low-temperature phase contains an asymmetrically bibridged linear chain of symmetrically bridged dimers and the high-temperature phase contains a tribridged chain.[15] The coordination geometry changes from square pyramidal to square bipyramidal. Thus the coordination number *increases* from 5 to 6 as the temperature is raised. In the low-temperature phase, the nonbridging chloride ions of the dimer are involved in strong N–H···Cl hydrogen bonds. This is weakened by the onset of a dynamic twofold disorder of the IPA ions above the phase transition temperature. These chloride ions then find it preferable to participate in asymmetrical bridges to adjacent

*To whom correspondence should be addressed at Hewlett-Packard, Disc Memory Division, Boise, Idaho 83707.

(1) L. Helmbolz and R. F. Kruh, *J. Am. Chem. Soc.* **74**, 1176 (1952).
(2) R. Gaura, C. P. Landee, R. D. Willett, H. Groenendijk, and A. J. van Duyneveldt, *Physica A (Amsterdam)*, submitted for publication. L. Antolini, G. Marcotrigiano, L. Menabue, and G. C. Tellacani, *J. Am. Chem. Soc.*, **102**, 1303, (1980).
(3) J. P. Steadman and R. D. Willett, *Inorg. Chim. Acta*, **4**, 367 (1970).
(4) R. L. Harlow, W. J. Wells III, G. W. Watt, and S. H. Simonsen, *Inorg. Chem.*, **13**, 2106 (1974).
(5) K. N. Raymond, D. W. Meek, and J. A. Ibers, *Inorg. Chem.*, **7**, 1111 (1968).
(6) R. E. Caputo, M. J. Vukosavich, and R. D. Willett, *Acta Crystallogr., Sect. B*, **B32**, 2516 (1976).
(7) R. M. Clay, P. Murray-Rust, and J. Murray-Rust, *J. Chem. Soc., Dalton Trans.*, 595 (1973).
(8) H. Remy, and R. Laves, *Ber. Dtsch. Chem. Ges. A*, **66**, 401 (1933).
(9) R. L. Harlow and S. H. Simonsen, ACA Abstracts.
(10) D. N. Anderson and R. D. Willett, *Inorg. Chim. Acta*, **8**, 167 (1974).
(11) G. C. Pellacani, to be submitted for publication.
(12) R. D. Willett, J. A. Haugen, J. Lebsach, and J. Morrey, *Inorg. Chem.*, **13**, 2510 (1974).
(13) R. D. Willett, J. R. Ferraro, and M. Choca, *Inorg. Chem.*, **13**, 2919 (1974).
(14) G. Marcotrigiano, L. Menabue, and G. C. Pellacani, *Inorg. Chem.*, **15**, 2333 (1976).
(15) S. A. Roberts, D. R. Bloomquist, R. D. Willett and H. W. Dodgen, *J. Am. Chem. Soc.*, submitted for publication.

0002-7863/81/1503-2615$01.25/0